

Volume 7, No. 2; April 2019

Advances in Image And Video Processing

ISSN: 2054-7412

TABLE OF CONTENTS

EDITORIAL ADVISORY BOARD	I
DISCLAIMER	II
The Patterns of Distribution of the Azimuth of the Winds at the Stage of Growth the Leaves of the Birch in the Vegetation Periods 2014 and 2018 Mazurkin P.M., Kudryashova A.I	1
Effect of Coordinate Birch at Automobile Roads on the Average Time of Vegetation and Maximum Width of Accounting Leaves Mazurkin P.M., Kudryashova A.I	9
Regularities of the Dynamics of the Average Width of the Leaves of Silver Birch Near the Maximum Growth in the Vegetation Period Mazurkin P.M., Kudryashova A.I	17
Improving Dynamic Parallel MRI Reconstruction via a Kernel-Based Learning Technique Yuchou Chang	25

EDITORIAL ADVISORY BOARD

Editor in Chief

Dr Zezhi Chen

Faculty of Science, Engineering and Computing
Kingston University London
United Kingdom

Professor Don Liu

College of Engineering and Science, Louisiana Tech
University, Ruston,
United States

Dr Lei Cao

Department of Electrical Engineering, University of
Mississippi,
United States

Professor Simon X. Yang

Advanced Robotics & Intelligent Systems (ARIS)
Laboratory, University of Guelph
Canada

Dr Luis Rodolfo Garcia

College of Science and Engineering, Texas A&M
University, Corpus Christi
United States

Dr Kyriakos G Vamvoudakis

Dept of Electrical and Computer Engineering, University
of California Santa Barbara
United States

Professor Nicoladie Tam

University of North Texas, Denton, Texas
United States

Professor Shahram Latifi

Dept. of Electrical & Computer Engineering University of
Nevada, Las Vegas
United States

Professor Hong Zhou

Department of Applied Mathematics Naval Postgraduate
School Monterey, CA
United States

Dr Yuriy Polyakov

Computer Science Department, New Jersey Institute of
Technology, Newark
United States

Dr Rodney Weber

School of Mathematics and Statistics
University College, Australian Defence Force Academy,
Australia

Dr Cornelia Laule

Dept. of Pathology and Laboratory Medicine
The University of British Columbia
Canada

Dr Yiqiang Q. Zhao

School of Mathematics and Statistics
Carleton University, Ottawa, Ontario
Canada

Dr Farouk YALAOUI

LOSI(Optimization Laboratory of Industrial Systems)
University of Technology of Troyes
France

Dr Daniel Berrar

School of Biomedical sciences
Ulster University
United Kingdom

Dr Ozlem Uzuner

Department of Information Studies
State university of New York
United States

Dr Erik L. Ritman

Psychology and Biomedical Engineering, Mayo Clinic,
State of Minnesota
United States

Dr Pascal Hitzler

Dept. of Computer Science and Engineering
Wright State University
United States

Dr Thomas D. Parsons

Dept. of Psychology
University of North Texas
United States

Dr Eric Hoffman

Department of Radiology
University of Iowa,
United States

Dr Salil Kanhere

Department of Computer Science and Engineering
University of New South Wales
Australia

Dr Maolin Tang

Department of Electrical Engineering and Computer
Science, Queensland University of Technology
Australia

Dr Simon X. Yang

Department of Engineering
University of Guelph
Canada

Dr Francisco Sepulveda

Department of Computer Science
University of Essex
United Kingdom

Dr Yutaka Maeda

Department of Electrical and Electronics Engineering
Kansai University
Japan

Dr Chin-Diew Lai

Department of Statistics
Massey University
New Zealand

Dr Ibrahim Ozkan

Department of Economics
Hacettepe University, Turkey

Dr Henry Schellhorn

Institute of Mathematics Sciences
Claremont Graduate University,
United States

Dr Laurence Devillers
Informatics Laboratory for Mechanics and Engineering
Sciences, University of Paris
France

Dr Stefan Kopp
Social Cognitive Systems Group, Bielefeld University
Germany

Dr A. K. Louis
Institute for Numerical and Applied Mathematics,
Saarland University
Germany

Dr Barry O'Sullivan
University College Cork (UCC)
Ireland

Dr Sabato Manfredi
University of Naples Federico
Italy

Dr Sergio Baragetti
Machine Design and Computational Mechanics
University of Bergamo, Italy

Dr Itamar Ronen
Department of Radiology
Leiden University Medical Centre
Netherlands

Dr Elli Androulaki
Zurich Research Laboratory, Zurich
Switzerland

Dr Jonathan Vincent
Department of IT
Bournemouth University
United Kingdom

Dr Gerard McKee
School of Systems Engineering
University of Reading
United Kingdom

Dr Jun Hong
Department of Computer Science
Queen's University Belfast
United Kingdom

Dr. Ig-Jae Kim
Imaging Media Research Center, Korea Institute of
Science and Technology, Seoul
South Korea

Dr. Reinhard Klette
School of Engineering, Computer and Mathematical
Sciences, Auckland University of Technology
New Zealand

Dr. Constantine Kotropoulos
Department of Informatics, Aristotle University of
Thessaloniki
Greece

Dr. Jun Ohta
Graduate School of Materials Science, Nara Institute of
Science and Technology (NAIST)
Japan

Prof. Klaus Hanke
Surveying and Geoinformation Unit
University of Innsbruck
Austria

Dr Jeff Schneider
School of Computer Science
Carnegie Mellon University,
United States

Dr Alexander J. Smola
Machine Learning Department
Carnegie Mellon University
United States

Dr Debmalya Panigrahi
Department Computer Science
Dule University
United States

Dr Chuck Jacobs
Machine Learning Group, Microsoft
United States

Dr Geoffrey Zweig
Natural Language Processing Group
JP Morgan
United States

Dr Gang Wang
Department of Computer Science
University of California, Santa Barbara
United States

Dr Christino Tamon
Department of Computer Science
Clarkson University
United States

Dr Paul S. Rosenbloom
Department of Computer Science
University of Southern California
United States

Dr Babak Forouraghi
Department of Computer Science
Saint Joseph's University
United States

Dr Haibo He
Department of Electrical, Computer, and Biomedical
Engineering, University of Rhode Island
United States

Dr. Ibrahim Abdulhalim
Department of Electro-Optics Engineering,
Ilse Katz Institute for Nanoscale Science and
Technology, Ben Gurion University
Israel

Prof. Dr. Erik Cuevas
Department of Electronics, Universidad de Guadalajara
Mexico

Prof. Dr. Bernard De Baets
KERMIT, Dept. of Mathematical Modelling Statistics and
Bioinformatics, Ghent University
Belgium

Dr. Joachim Denzler
Computer Vision Group, Institute for Informatics
Friedrich-Schiller-University Jena
Germany

Dr. Antonio Fernández-Caballero
Universidad de Castilla-La Mancha
Spain

DISCLAIMER

All the contributions are published in good faith and intentions to promote and encourage research activities around the globe. The contributions are property of their respective authors/owners and the journal is not responsible for any content that hurts someone's views or feelings etc.

The Patterns of Distribution of the Azimuth of the Winds at the Stage of Growth the Leaves of the Birch in the Vegetation Periods 2014 and 2018

Mazurkin P.M.¹, Kudryashova A.I.².

¹Dr. Sc., Prof., Volga State University of Technology, Yoshkar-Ola, Russia, e - mail:

²S. lec., Volga State University of Technology, Yoshkar-Ola, Russia, e - mail:

kaf_po@mail.ru; Little-one7@yandex.ru

ABSTRACT

Formation and death of leaves in the cycle of ontogenesis are divided into the following stages: Bud growth and development of leaves, blooming dying leaves, leaf subsidence. We propose two more stages of ontogenesis – growth to the maximum and decline to the fall. The stage of growth of birch leaves hanging to the maximum width (similar to the length, area and perimeter of the leaves) of the growing season becomes a great quantum of plant behavior. This quantum with high adequacy shows that on three-time measurements of wind azimuth the distribution of the number of wind directions occurs according to the superstrong laws in 2014 and 2018. Then a three-hour quanta measurements of the azimuth of the winds make it very high to determine the adequacy of distribution of measurement directions of the wind. In 2014 had arisen three prevailing directions, growth of incidence azimuth: 45, 202.5 and 337.50. And in 2018 there were two directions of prevailing winds: 67.5 and 2700 in the city of Yoshkar-Ola. The three-hour distribution of wind directions along the azimuth at the first stage of the growing season of birch leaves from the first of may to August 20 of each year occurs according to clear laws, including wave equations with variable amplitude, changing according to the biotechnical law. For 2018, seven waves with a half-period of oscillations in the 45.1, 27.7, 23.25, 24.17, 0.23, 22.65 and 723 days. Of these, a constant period of $2 \times 24.17 = 48.3$ days.

Key words: vegetation, growth stage to maximum, width, prevailing winds, wind azimuths, distributions, vibrational adaptation, regularities

1 Introduction

Climate change affects the vegetation of the Earth. In Finland, there is an indication of the reaction of young deciduous trees to rising air temperatures in interaction with tropospheric ozone. This knowledge increases the chances of developing models to include parameters that describe the forest system in changing climatic conditions [9]. It can be argued that the future of CO₂ containment lies in an increase in the area, primarily forests [10, 11]. The dynamics of carbon in Europe changes according to wavelets of universal design [7, 8]. In Berlin [1] 252 the tree of lime in the cores by the distance from the center to the periphery was revealed changes of the increment of the thickness of the trees for 50 to 100 years.

The understanding of modeling of mutual relations between the parameters of the plant leaf structure by the method of identification [5-7] comes. A priori it is clear that the weather affects the course of development and growth (ontogenesis) of plants. And perennials weather is affected through annual

DOI: 10.14738/aivp.72.6688

Publication Date: 06th June, 2019

URL: <http://dx.doi.org/10.14738/aivp.72.6688>

ontogenesis of leaves. The quanta of leaf behavior, for example, of the birch tree, widespread in the Northern hemisphere [15], clearly depend on the quanta (asymmetric wavelets [7, 8]) behavior of air temperature and relative humidity. Meteorological conditions are strong factors of activity of biological objects, and for this purpose in article [3] influence of temperature, precipitation, atmospheric pressure and humidity on phenology of amphibians in South-East Queensland (Australia) is estimated.

Plant growth is a complex process, it is based on such fundamental phenomena as rhythm, polarity, differentiation, irritability, correlation. These processes are common for ontogenesis. Ontogenesis – individual development of the body from zygote (or vegetative germ) to natural death. Because of the photosynthetic activity of the leaves, the plant acquires a number of features that characterize its growth. In the process of plant ontogenesis growth is observed during the main stages of its life cycle [2, 4, 10].

Formation and death of leaves in the cycle of ontogenesis are divided into the following stages: Bud growth and development of leaves, blooming dying leaves, leaf subsidence. We propose two more stages of ontogenesis – growth to the maximum and decline to the fall.

The growing season is becoming one of the important ecosystem processes, as the development of leaves is very sensitive to air temperature. Therefore, the future of climate is in leaf observations [11]. The metric parameters of the leaves depend on the growing season.

Birch hanging in Estonia proved to be effective against drought in 2010. Trees adapt well, and the importance of relative humidity is even higher compared to air temperature [13]. Increasing humidity reduces the temperature and biomass accumulation in young birches, especially susceptible leaves [14].

The purpose of the article is to improve the accuracy of the indication under patent 2606189 the invention of the quality of the surrounding birch leaves of the local environment on the side at a height of 1.5 -2.0 m from the prevailing winds on the dynamics of the average width of 10 leaves in different environmental conditions of growth near the road with heavy traffic cars.

2 Materials and methods

The longest growing season since Bud break (may 2, 2014 and may 1, 2018) to the maximum leaf width was 111 days in 2014 (August 20) and 110 days in 2018 (August 18). For growth stages (Fig. 1) we accept dates from 01.05 to 20.08 and in three hours we will write down the data "wind Direction (Rumba) at an altitude of 10-12 meters above the earth's surface" for the weather station Yoshkar-Ola. Then the cells with "Calm" were excluded from the data array, and the Rumba were converted into azimuth.

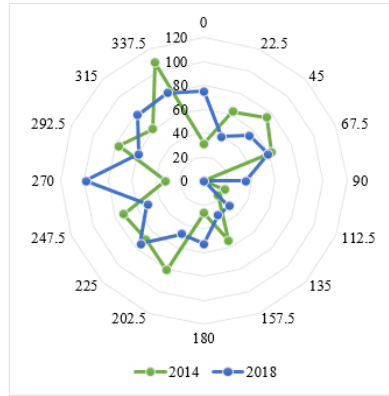


Figure 1. Wind rose in Yoshkar-Ola at the stage of growth during the growing season, birch hanging from 01.05 to 20.08

In four years, the direction of prevailing winds shifted from 337.50 to 270.0. Then it can be argued that the direction of the winds is near the North-West.

Chart data in figure 1 are shown in table 1. Here are the residues (absolute error), as the difference between the actual and the calculated wave equations (table 2). And also in table 1 the values of the relative error are given, as the ratio (in percent) in the form of dividing the residues by the actual values of the wind azimuth.

Table 1. The direction of the winds at the stage of growth the leaves of the silver birch

Azimuth φ , degree	The number N of rhombuses in wind direction units					
	Year 2014	Tailings	Error	Year 2018	Tailings	Error
0	31	-0.210962	-0.68	75	0.104856	0.14
22.5	63	0.50304	0.80	40	-0.0268786	-0.07
45	75	-0.714944	-0.95	54	0.0306427	0.06
67.5	62	0.227208	0.37	58	-0.0357718	-0.06
90	0	0.196342	-	35	0.0314459	0.09
112.5	19	-0.00369648	-0.02	0	-0.0262315	-
135	17	-0.101437	-0.60	30	0.0266313	0.09
157.5	54	0.227061	0.42	31	0.000856083	0.00
180	27	0.590869	2.19	53	0.00342509	0.01
202.5	81	0.0897795	0.11	48	-0.0138827	-0.03
225	69	0.0673064	0.10	75	0.00819107	0.01
247.5	73	-0.0758387	-0.10	51	-0.011106	-0.02
270	32	-0.306591	-0.96	99	0.0205141	0.02
292.5	77	0.0334596	0.04	59	-0.0272314	-0.05
315	61	-0.0182502	-0.03	78	0.0145546	0.02
337.5	107	-0.455811	-0.43	80	-0.0386905	-0.05
Just	848			866		

Oscillations(wavelet signals) are recorded by the wave formula [14-17] of the form

$$y_i = A_i \cos(\pi x / p_i - a_{8i}), A_i = a_{1i} x^{a_{2i}} \exp(-a_{3i} x^{a_{4i}}), p_i = a_{5i} + a_{6i} x^{a_{7i}}, \quad (1)$$

where y – the index (dependent factor), i – номер components of the model (1), m – number of members in the model (1), x – explanatory variable (influencing factor), $a_1...a_8$ – the parameters of the model (1) taking the numerical values in the course of structural-parametric identification in the

software environment Curve Expert-1.40 (URL: <http://www.curveexpert.net/>), A_i – amplitude (half) of wavelet (axis y), p_i – the half-period fluctuations (axis x).

3 Results and discussion

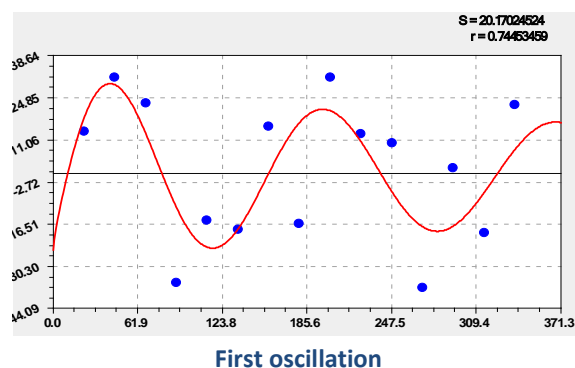
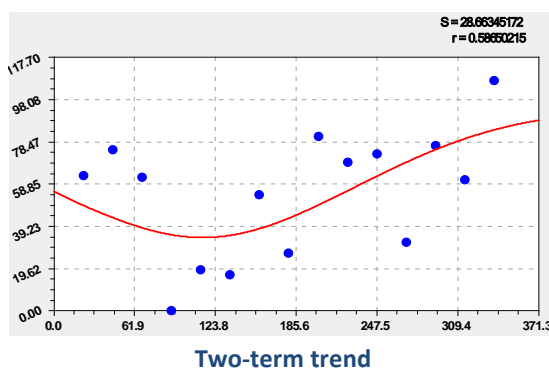
Table 2 gives the parameters (1) according to table 1.

Table 2. Options (1) directions of the wind azimuths in growing birch leaves

Number i	Wavelet $y_i = a_{1i}x^{a_{2i}} \exp(-a_{3i}x^{a_{4i}}) \cos(\pi x / (a_{5i} + a_{6i}x^{a_{7i}}) - a_{8i})$								Coef. corr. r
	The amplitude (half) the fluctuations				The half-period of oscillations			Shift	
	a_{1i}	a_{2i}	a_{3i}	a_{4i}	a_{5i}	a_{6i}	a_{7i}	a_{8i}	
Growth stage of the growing season 2014									
1	31.04888	0	-0.0022750	1	0	0	0	0	0.8559
2	4.06016e-18	26.00798	56.02962	0.11207	0	0	0	0	
3	43.62256	0	0.00025496	1.51089	-439.5006	479.37559	0.016749	1.61580	0.5645
4	-0.24363	1.10734	0.0094773	1	41.19066	0	0	1.12850	
5	8.84433e-7	3.96058	0.011097	1.10024	26.21567	-0.00019902	1.67304	1.62260	0.9919
6	-3.00032e-26	13.75107	0.063782	1.00350	43.87951	0.00014347	1.84964	0.061472	0.7472
7	4.56629	0	0.014893	1	72.84731	-0.013148	1	-1.08682	0.9478
Growth stage of the growing season 2018									
1	84.77647	0	0.011844	1	0	0	0	0	0.8895
2	9.43003e6	41.69824	96.48688	0.16659	0	0	0	0	
3	32.51765	0	0.0071364	1	45.13786	0.00018205	2.04081	4.43375	0.9865
4	-4.32383e-13	7.19338	0.0060364	1.29657	27.72950	-0.00045090	1.62188	-4.77571	
5	-1.35019	0	-0.00039237	1.34949	23.24999	0.057855	0.99288	5.47970	0.9551
6	-0.36915	0.035157	0.00012797	1.36144	24.16514	0	0	-0.31166	0.4996
7	-1.41559	0.047326	0.0062964	1	0.23369	0.024887	1	5.71216	0.7413
8	4.71860	17.24510	0.073747	1.00392	22.64515	0.027914	0.98229	1.69285	0.9329
9	1.71127e-6	5.45479	0.56047	0.61560	722.97994	6.84720	1.18444	-1.45528	0.9157

The first term models with parameters from table 2 is the law of Laplace (in math), Mandelbrot (in physics), texts-pearl (biology) and Pareto (econometrics). But different directions: for 2014 it is the law of exponential growth, and for 2018 – exponential death. This natural law changes for wind directions depending on the azimuth with correlation coefficients 0.5865 and 0.8000. This fact indicates that the growth stage of the growing season of 2018 was better in wind directions. The second term of the trend is a biotechnical law [14]. All vibrations have a very high value. It is this property of oscillation that indicates that plants have adapted to wave changes in meteorological parameters over hundreds of millions of evolutions.

Figures 1 and 2 show graphs of all components of the General model (1).



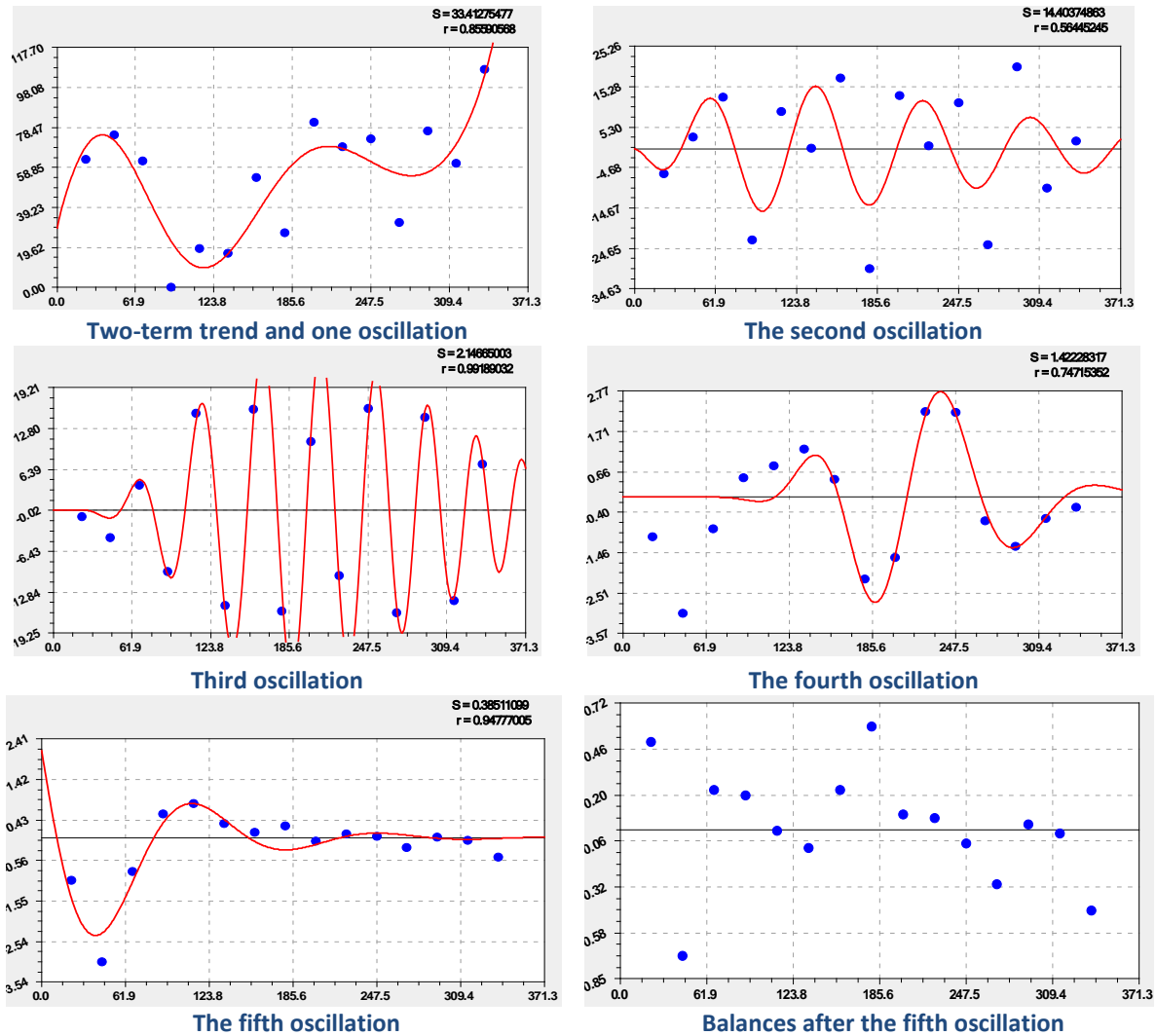
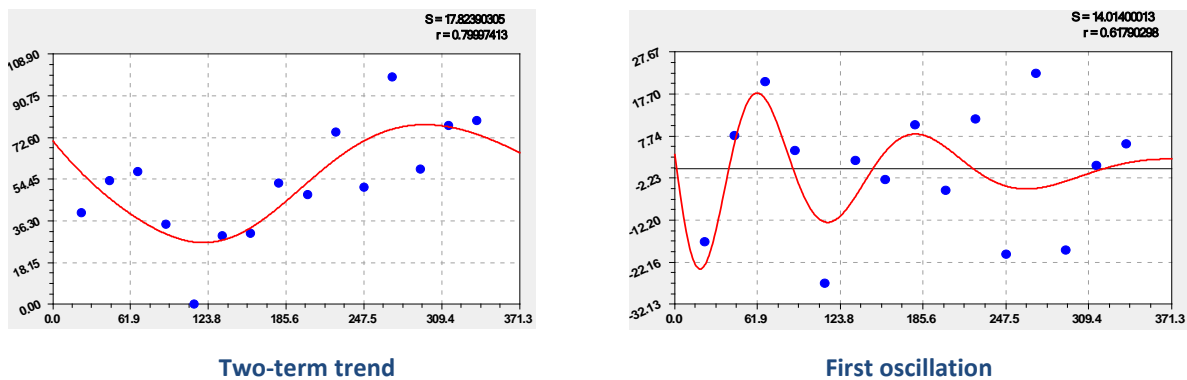


Figure 1. Graphics wavelets of the directions of the wind in 2014, the growth stage of the leaves

The maximum relative error in table 1 is 2.19% for 2014 and 0.14% for 2018. At the same time, the first three members obtained by the capabilities of the Curve Expert-1.40 software environment received a correlation coefficient of 0.8559 and 0.8859. All five fluctuations in the growth phase of 2014 ended before August 20, when there was a maximum of average width.

For the growth phase in 2018 (Fig. 2) there were seven oscillations.

Of these, only the fourth oscillation continued after 20.08. The fifth oscillation shows that the growing season began in the directions of winds spontaneously, and then the period of oscillation increased.



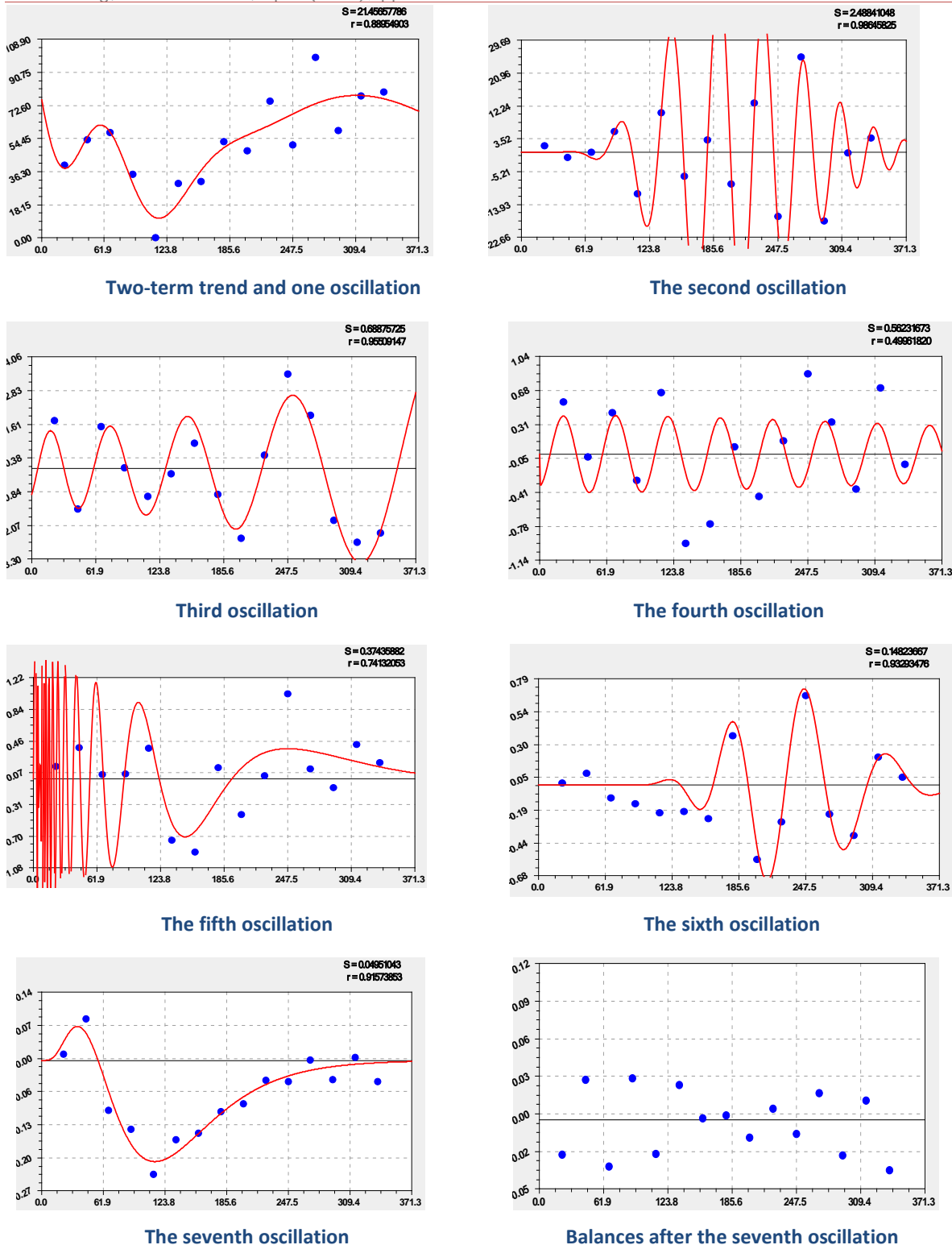


Figure 2. Graphics wavelets of the directions of the wind in 2018, at the growth stage of the leaves

The law of stress excitation for the second term from table 2 shows that, apparently, the wind direction stimulates the growth of vegetative organs of plants. This was facilitated by the third oscillation (fifth term) with a correlation coefficient of 0.9919 in 2014. And in 2018, the strengthening of the vibrational adaptation of leaf growth was due to the second member (biotechnical law) and the fourth member of the strongest adequacy (0.9865).

Thus, we have proved that the three-hour distribution of wind directions along the azimuth at the first stage of the vegetation period of birch leaves from the first of May to August 20 of each year occurs according to clear laws, including wave equations with variable amplitude, changing according to the biotechnical law.

The period of oscillation varies in a wide range. It is not clear why the first fluctuation in 2014 occurred with a negative period of $2 \times (-439.5) = -879$ days. The remaining waves had periods of 82.4, 52.4, 87.8 and 145.7 days. Half-life of 41.2 days is constant for the whole stage of leaf growth in 2014 and is close to 40 days of weather.

For 2018, seven waves with a half-period of oscillations in the 45.1, 27.7, 23.25, 24.17, 0.23, 22.65 and 723 days. Of these, a constant period of $2 \times 24.17 = 48.3$ days. Start account leaves the latest fluctuation shows that the maximum half life for 01.05.2018 the wind directions is equal to 723 days. The stage of growth of birch leaves in 2018 was more complicated than in 2014 due to the emergence of the fifth and seventh oscillations. Such uncertainties are likely to increase in the future.

Analysis of the three charts shows that in 2014, there have been three prevailing wind directions, in ascending order of frequency of occurrence of the azimuth of the winds: 45, 202.5 and 337.5°. And in 2018, only two directions of prevailing winds were formed: 67.5 and 270°. It is characteristic that out of 848 wind directions at the stage of growth of birch leaves in 2014 there was not a single case in the direction of the azimuth 90°, and in 2018 zero events out of 866 – in the azimuth 112.5°.

4 Conclusion

Thus, the stage of growth of birch leaves hanging to the maximum width (similar to the length, area and perimeter of the leaves) of the growing season is a great quantum of plant behavior. This quantum with high adequacy shows that according to the three-hour measurement of the wind azimuth, the distribution of the number of wind directions occurs according to super-strong laws in 2014 and 2018. Then a three-hour quanta measurements of the azimuth of the winds make it very high to determine the adequacy of distribution of measurement directions of the wind.

In 2014, there were three predominant directions in the growth of azimuth occurrence: 45, 202.5 and 337.5°. And in 2018 there were two directions of prevailing winds: 67.5 and 270°.

REFERENCES

- [1] Dahlhausen J. et al. Urban climate modifies tree growth in Berlin. International Journal of Biometeorology (2018) 62:795–808. <https://doi.org/10.1007/s00484-017-1481-3>.
- [2] Does humidity trigger tree phenology? Proposal for an air humidity based framework for bud development in spring // New Phytologist (2014) 202: 350–355. 2014 The Authors www.newphytologist.com.
- [3] Calling phenology of a diverse amphibian assemblage in response to meteorological conditions / T.L. Plenderleith, et.al.Hero.International Journal of Biometeorology.(2018). 62:873–882. <https://doi.org/10.1007/s00484-017-1490-2>.
- [4] Y.H. Fu, et al. Declining globalwarming effects on the phenology of Spring leaf unfolding. Letter. 2015. Vol 526. Nature / doi:10.1038/nature15402.
- [5] P.M. Mazurkin.Method of identification.(2014). International Multidisciplinary Scientific GeoConference Surveying Geology and Mining Ecology Management.SGEM.1 (6). pp. 427-434.

- [6] P.M. Mazurkin. Identification of the wave patterns of behavior. (2014). *International Multidisciplinary Scientific GeoConference Surveying Geology and Mining Ecology Management.SGEM.1* (6). pp. 373-380.
- [7] P.M. Mazurkin. Wavelet Analysis Statistical Data. *Advances in Sciences and Humanities*. Vol. 1.No. 2. 2015. pp. 30-44. doi: 10.11648/j.ash.20150102.11.
- [8] P.M. Mazurkin. A.I. Kudryashova. Factor analysis of annual global carbon dynamics (according to Global_Carbon_Budget_2017v1.3.xlsx). *Materials of the International Conference "Research transfer" - Reports in English (part 2)*. November 28. 2018. Beijing.PRC.P.192-224.
- [9] M. Maarit. Impacts of temperature and ozone on carbon retention processes of birch and aspen *Dissertations in Forestry and Natural Sciences*. Finland.Joensuu.on June. 08. 2012.54 p.
- [10] Mapping tree density at a global scale / T. W. Crowther.et. al. *Nature* 525.201–205 (2015); doi:10.1038/nature14967. 13 p.
- [11] C.A. Polgar, R.B. Primack. Leaf-out phenology of temperate woody plants: from trees to ecosystems // *New Phytologist* (2011) 191: 926–941. doi: 10.1111/j.1469-8137.2011.03803
- [12] M. Rousi, J. Pusenius/ Variations in phenology and growth of European white birch (*BetulaPendula*) clones // 2005. *Heron Publishing—Victoria, Canada. Tree Physiology* 25, 201–210/
- [13] Sellin A. et al. Rapid and long-term effects of water deficit on gas exchange and hydraulic conductance of silver birch trees grown under varying atmospheric humidity. *BMC Plant Biology*. 2014, 14:72. <http://www.biomedcentral.com/1471-2229/14/72>.
- [14] Sellin A. et al. Elevated air humidity affects hydraulic traits and tree size but not biomass allocation in young silver birches (*Betulapendula*). *Frontiers in Plant Science*.October 2015 | Volume 6 | Article 860.doi: 10.3389/fpls.2015.00860.
- [15] A.L. Takhtajan. *Floristic Regions of the World*. Berkeley-Los Angeles-London: University of California press, 1986. 523 p.

Effect of Coordinate Birch at Automobile Roads on the Average Time of Vegetation and Maximum Width of Accounting Leaves

Mazurkin P.M.¹, Kudryashova A.I.².

¹Dr. Sc., Prof., Volga State University of Technology, Yoshkar-Ola, Russia, e - mail:

²S. lec., Volga State University of Technology, Yoshkar-Ola, Russia, e - mail:

kaf_po@mail.ru; Little-one7@yandex.ru

ABSTRACT

For environmental assessment of the quality of the surrounding growing birch area in the summer of 2018, the width of 10 leaves of 10 birch trees hanging in the city of Yoshkar-Ola was measured. The distances from the edge of the road to the center of the birches were measured, as well as the height of the crown zone at each birch from the prevailing winds. The geographical coordinates of the trunk axis were measured by the cell phone, which were given to the conditional Northern latitude and Eastern longitude. From these influencing factors regularities of change of time of a Vegetation since may 1 and average maximum width of accounting leaves were received. The factor analysis of six influencing variables and two dependent indicators is carried out. Formulas and graphs are given. It is found that the influence of the distance from the road on the maximum width of the leaves has a correlation coefficient 0.7574, and the influence of the reduced East longitude on the same biometric parameter 0.7514. The average maximum width of the birch leaves can be a great indicator of pollution of the roadside area. To identify wave patterns, it is necessary to take more than 20 birches in different places.

Key words: vegetation of leaves, growth stage to the maximum, prevailing winds, 10 birches, 10 leaves, width, road, coordinates, trends, oscillatory adaptation, patterns

1 Introduction

It can be argued that the future of CO₂ containment lies in an increase in the area, primarily forests [8, 9]. The dynamics of carbon in Europe changes according to wavelets of universal design [6, 7].

In ecological technologies with the use of birch leaves, the understanding of modeling of mutual relations between the parameters of the leaf structure by the identification method [5, 6] comes. A priori it is clear that the weather affects the course of development and growth (ontogenesis) of plants. And perennials weather is affected through annual ontogenesis of leaves. The quanta of leaf behavior, for example, of the birch tree, widespread in the Northern hemisphere, clearly depend on the quanta (asymmetric wavelets [6, 7]) behavior of air temperature and relative humidity. Meteorological conditions are strong factors of activity of biological objects, and for this purpose in article [3] influence of temperature, precipitation, atmospheric pressure and humidity is estimated.

Plant growth is a complex process, it is based on such fundamental phenomena as rhythm, polarity, differentiation, irritability, correlation. These processes are common for ontogenesis of living organisms [2, 4, 8]. **Ontogenesis** – individual development of the body from zygote (or vegetative germ) to natural death. Thanks to the active activity of meristems and photosynthetic activity of leaves, the green plant acquires a number of features that characterize its growth. In the process of plant ontogenesis growth is observed during the main stages of its life cycle [12, 15].

Formation and death of leaves in the cycle of ontogenesis are divided into the following stages: Bud growth and development of leaves, blooming dying leaves, leaf subsidence. We propose two stages of ontogenesis – growth to the maximum and decline to the fall.

In Berlin [1] 252 the tree of lime in the cores by the distance from the center to the periphery was revealed changes of the increment of the thickness of the trees for 50 to 100 years. Seven tree species in Europe [14] showed nonlinear dependence of plant development on temperature and microclimate. There is still uncertainty in Biometeorology for the future. The influence of urban vegetation on human thermal comfort equal to 22.2 °C is shown in [13]. A rational phytoclimate will help to counteract global warming.

The growing season is becoming one of the important ecosystem processes, as the development of leaves is very sensitive to air temperature. Therefore, the future of climate is in leaf observations [9]. Increasing humidity reduces the temperature and biomass accumulation in young birches, especially susceptible leaves [11].

The purpose of this article is to increase the accuracy of indication of the quality of the surrounding birch leaves local environment side at a height of 1.5 to 2.0 m from the side of the prevailing winds at the time of the growing season in 2018 from the first of may to the maximum width as the average of the 10 account if-stew the patent for the invention 2606189 depending on the distance from the edge of the road high you the location of the center of the zone 10 account leaves over the soil and given the geographical-ray coordinates of the location of the center of the butt end of trees.

2 Materials and methods

The oscillations are recorded by the wave formula [5, 6] of the form

$$y_i = A_i \cos(\pi x / p_i - a_{8i}), \quad A_i = a_{1i} x^{a_{2i}} \exp(-a_{3i} x^{a_{4i}}), \quad p_i = a_{5i} + a_{6i} x^{a_{7i}}, \quad (1)$$

where y – the index (dependent factor), i – number components of the model (1), m – number of members in the model (1), x – explanatory variable (influencing factor), $a_1 \dots a_8$ – the parameters of the model (1) taking the numerical values in the course of structural-parametric identification in the software environment Curve Expert-1.40 (URL: <http://www.curveexpert.net/>), A_i – amplitude (half) of wavelet (axis y), p_i – the half-period fluctuations (axis x).

Table 1 shows the distances from the road and soil, as well as the geographical and biometric parameters of 10 birches in Yoshkar-Ola on the average width of 10 leaves.

Table 1. Birch trees location parameters with 10 checklists on each tree

Place record birches	Distances L and h , m		Coordinate System birches		Reduced coordinates system 1 $0^{\circ}, 0^{\circ}$		Time vegetations τ , day	Maximum width, \bar{b}_{max} , mm
	road	soil	Northern latitude	Eastern longitude	Northern latitude α	Eastern longitude β		
1. Lebedev Street	7.0	1.60	56°37' 6"	47°56' 48"	1.833	14.667	110	45.92
2. Voskresensky pros.	2.9	1.46	56°38' 6"	47°54' 51"	3.500	11.417	110	48.66
3. Street Eshkinina	5.2	1.40	56°37' 58"	47°54' 47"	3.278	11.306	92	39.77
4. Lenin avenue	4.9	1.60	56°38' 8"	47°53' 12"	3.556	8.667	99	40.11
5. Chawain Boulevard	2.1	1.60	56°37' 52"	47°54' 47"	3.111	11.306	106	44.71
6. Panfilov Street	4.1	1.30	56°37' 40"	47°52' 55"	2.778	8.194	103	39.56
7. Karl Marx Street	3.2	1.60	56°36' 47"	47°52' 45"	1.306	7.917	99	44.39
8. Builders Street	4.3	1.45	56°36' 54"	47°52' 5"	1.500	6.806	103	42.25
9. Botanical garden	2.4	1.55	56°38' 42"	47°52' 50"	4.500	8.056	103	40.71
10. Osipenko Street	2.3	1.45	56°38' 42"	47°52' 50"	4.500	8.056	99	44.09

On each birch tree on the side of the crown from the prevailing winds (approximately North-West) there was a zone with a diameter of about 0.5 m, where 10 leaves were allocated, white threads with tags were tied to their tails, on which the numbers of the leaves were indicated. The reduced coordinate system was calculated as follows. With the help of a cell phone at first recorded the coordinates of the zone of accounting leaves (in degrees, minutes and seconds). Then these values resulted in degrees according to the formula $PC = \text{degree} + \text{minute} / 60 + \text{seconds} / 3600$. The results read: North latitude origin -56.6° ; East longitude origin -47.8° . However, for the Curve Expert 1.40 software environment, you must multiply the obtained values of the reduced coordinates by 100.

3 Results and discussion

Table 3 presents the results of the factor analysis according to table 1. Here are the factors L , h , α and β are the only influencing variables, so the horses can't become dependent parameters. The factors τ and \bar{b}_{max} become both influencing and dependent parameters, so they can be ranked by the pre-order vector of preference «better \rightarrow worse». For both of the biometric parameters τ and \bar{b}_{max} vector accepted «the more the better»

Then the rank distribution will obey the law of exponential death at ranks (Fig. 1) by formulas

- for the rank distribution of vegetation time of accounting leaves in 10 birches (0.9912)

$$\tau = 109.86894 \exp(-0.020293 R_r^{0.95603}); \tag{2}$$

- for an average width of 10 leaves for each of the 10 birch trees (0.9852)

$$\bar{b}_{max} = 48.51034 \exp(-0.044851 R_b^{0.70910}). \tag{3}$$

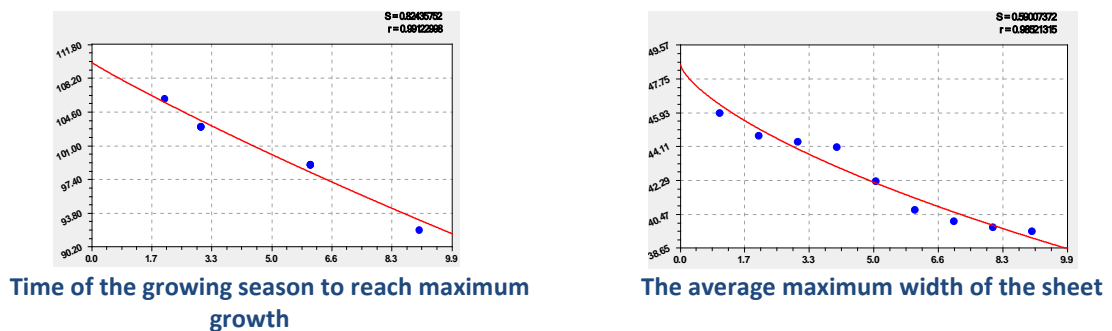


Figure 1. Graphs of rank distribution of biometric parameters of birch leaves

Table 2 shows the results of factor analysis using the trend as a special case of formula (1) with an infinite period of oscillation.

Table 2. Correlation matrix of factor analysis and rating of factors after identification by trend pattern

Influencing factors (characteristic x)	Dependent factors (indicators y)		Amount Σr	Place I_x
	τ , day	\bar{b}_{max} , mm		
Distance of the group leaves from the road L , m	0.0021	0.7574	0.7595	4
The height of the group leaves from the soil h , m	0.2360	0.4640	0.7000	5
Given the Northern latitude α , °	0.1582	0.1656	0.3238	6
East longitude given β , °	0.5326	0.7540	1.2866	3
Times of growth accounting leaves τ , day	0.9912	0.6804	1.6716	1
The average width of the leaves account \bar{b}_{max} , mm	0.6793	0.9852	1.6645	2
The sum of the correlation coefficients Σr	2.5994	3.8066	6.4060	-
Place I_y	2	1	-	0.5338

The coefficient of correlation variation, as a measure of the adequacy of the entire system of parameters of the object of study, is defined as $6.4060 / (6 \times 2) = 0.5338$. The first place among the influencing variables is the growing season until the end of the growth stage, and the second – the average width of the leaves at the maximum growth of leaves. Among the dependent indicators as evaluation criteria is the average width of the leaves at the end of the growth stage.

Choose the correlation matrix (tab. 3) with medium and strong binary relations with a correlation coefficient of at least 0.5. The greatest correlation coefficient 0.7574 has the effect of the distance from the approximate center of the zone of 10 leaves on the lateral surface of the crown of birch hanging from the prevailing winds (North-West) to the edge of the road.

Table 3. Correlation matrix with correlation coefficient not less than 0.5

Influencing factors (characteristic x)	Indicators y	
	τ , day	\bar{b}_{max} , mm
Distance of the group leaves from the road L , m		0.7574
East longitude given β , °	0.5326	0.7540
Times of growth accounting leaves τ , day		0.6804
The average width of the leaves account \bar{b}_{max} , mm	0.6793	

In table 4, we place the trend models in descending order of adequacy.

Table 4.Options trend binary relations data on table 1

Variable x	Indicator y	Trendy = $aexp(-bx^c) + dx^e exp(-fx^g)$							Coef. Corr. r
		Exponentiallaw			Biotechnicallaw				
		a	b	c	d	e	f	g	
L, m	\bar{b}_{max}, mm	0.27696	-4.90586	0.041252	-2.50694e7	25.06937	27.20913	0.43559	0.7574
$\beta, ^\circ$		47.77710	6.90355e-5	3.64290	8.14379e-140	185.8460	6.73438	1.21378	0.7514
τ, day		0	0	0	0.65415	0.90434	0	0	0.6804
\bar{b}_{max}, mm	τ, day	0	0	0	14.42463	0.52119	0	0	0.6793
$\beta, ^\circ$		204.11047	0.29180	1	30.74222	0.46543	0	0	0.5325

Figure 2 shows graphs of the effect of the distance from the road to the leaves.

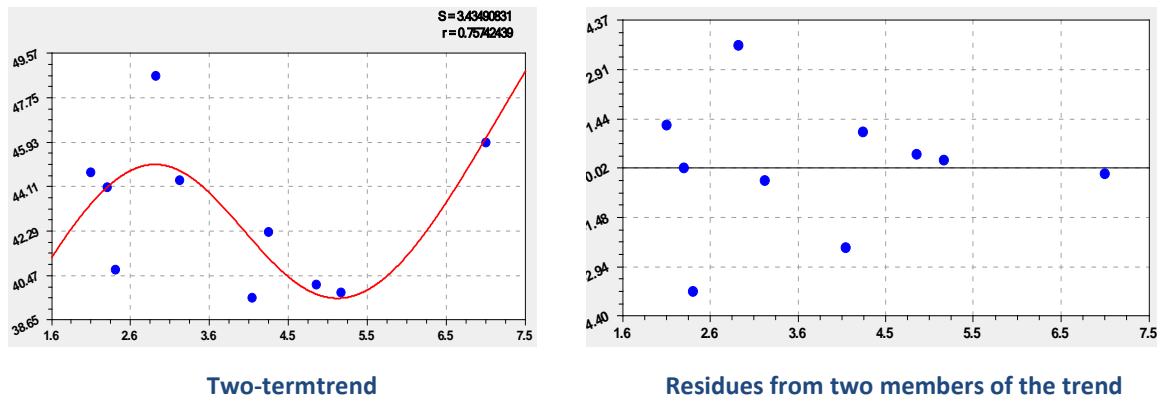


Figure 2. Graphs of the influence of the distance from the road on the average max. width of the leaf group

From the point chart of residues it can be seen that the oscillation is possible (tab. 5, Fig. 3). Due to the small number of points the correlation coefficient of the three-membered model became equal to 1.0000.

Table 5.Models (1) the effect of distance from the road on the max.of the average width of the sheet

Number i	Wavelet $y_i = a_{1i}x^{a_{2i}} \exp(-a_{3i}x^{a_{4i}}) \cos(\pi x / (a_{5i} + a_{6i}x^{a_{7i}}) - a_{8i})$								Coef. Corr. r
	The amplitude (half) the fluctuations				The half-period of oscillations			Shift	
	a_{1i}	a_{2i}	a_{3i}	a_{4i}	a_{5i}	a_{6i}	a_{7i}	a_{8i}	
1	5.77155	0	-1.96504	0.041252	0	0	0	0	1.0000
2	-5.59056e9	25.07757	30.15966	0.43558	0	0	0	0	
3	-3.34826e-20	174.83658	46.85684	1.02318	0.81421	4.65539e-5	4.22651	1.29874	
4	2308.83874	0	1.47595	1.73980	0.022770	0.021648	1.01222	3.29490	0.9523

The average maximum width of the birch leaves can be a great indicator of pollution of the roadside area. To identify wave patterns, it is necessary to take more than 20 birches in different places.

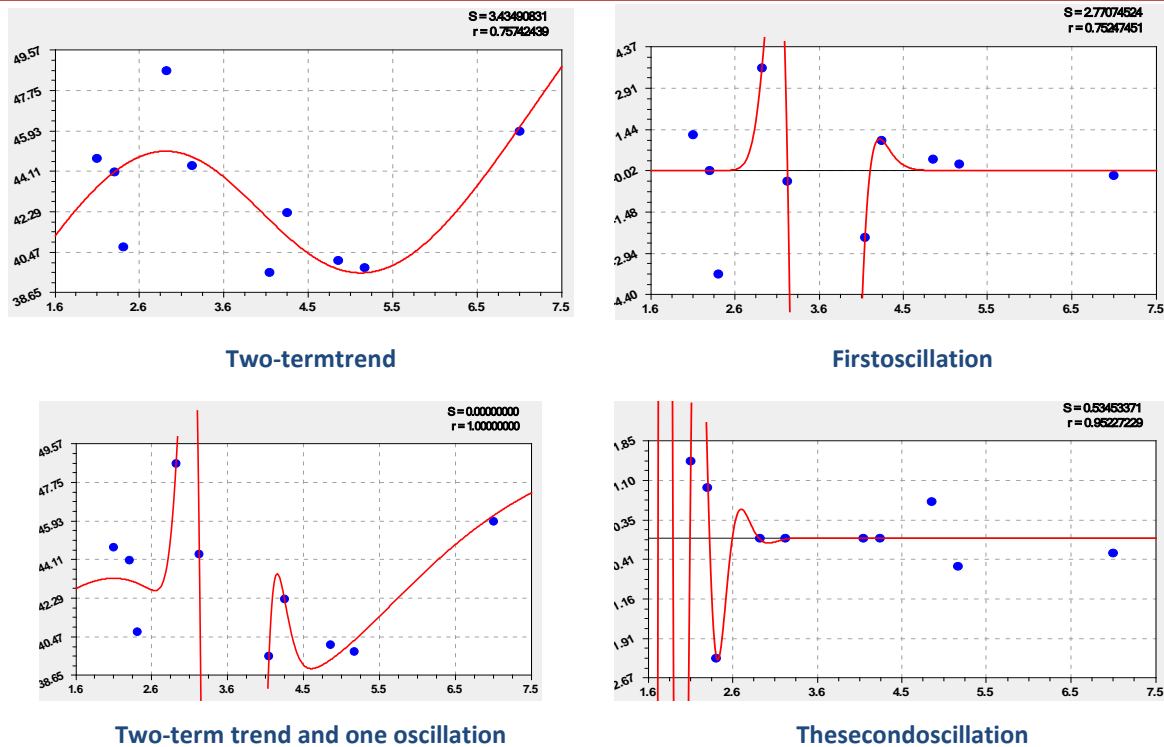


Figure 3. Graphs of the influence of the distance from the road on the average max. width of the leaf group

The greatest turbulence is observed up to 3 m from the edge of the road. Here, according to the trend, the maximum of the average width is observed. And then from 3 m to 5 m, there is a decrease in the width of the leaf, that is, in this distance from the road, there is a strong suppression of the vegetation of the leaves. After 5 m birch leaves begin to grow with the increasing width of the leaves.

The rest of the patterns from table 4 are shown in figure 4.

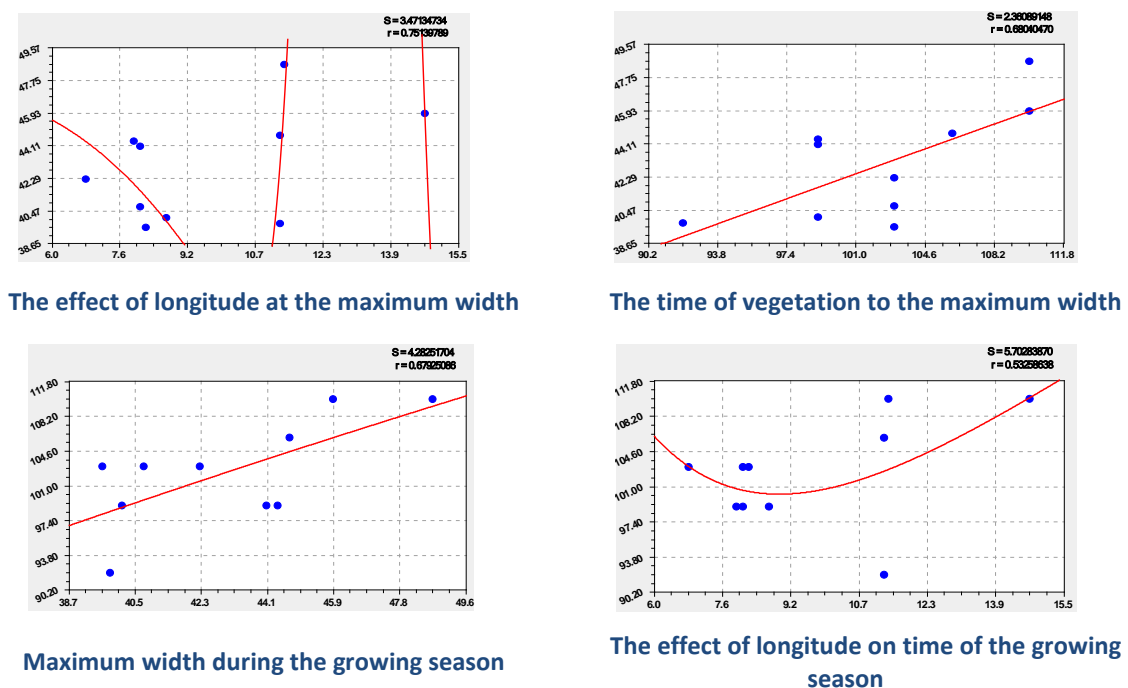


Figure 4. Graphs of binary relations according to table 4

Direct and reverse influence of biometric parameters of leaves according to table 4 occur according to the exponential law. Let's take a closer look at the influence of East longitude.

According to the schedule in figure 4, the decrease in vegetation time occurs in the Central district of Yoshkar-Ola. The most difficult way to change the schedule of long-term impact on the average maximum width of the leaves. Figure 5 shows a schematic map of 10 birch trees. It is seen that the main transect is obtained along the river Malaya Kokshaga.



Figure 5. Map-scheme of location of accounting 10 trees silver birch

Thus, the maximum width of the accounting leaves decreases from West to East on the right side of the city to the river, and on the left side of the river, the increment of the width of the leaves increases sharply, but again decreases in areas with high-rise buildings.

4 Conclusion.

The average maximum width of the birch leaves can be a great indicator of pollution of the roadside area. To identify wave patterns, it is necessary to take more than 20 birches in different places.

On each birch tree on the side of the crown from the prevailing winds allocated area where 10 accounting leaves, and to their roots tied white thread with tags and numbers. Cell phone recorded the coordinates of the zone of leaves. Then the given coordinates were calculated. For the Curve Expert 1.40 software environment, multiply the obtained values of the reduced coordinates by 100.

REFERENCES

- [1] Dahlhausen J. et al. Urban climate modifies tree growth in Berlin. *International Journal of Biometeorology*(2018) 62:795–808. <https://doi.org/10.1007/s00484-017-1481-3>.

- [2] Does humidity trigger tree phenology? Proposal for an air humidity based framework for bud development in spring // *New Phytologist* (2014) 202: 350–355 _ 2014 The Authors www.newphytologist.com.
- [3] Calling phenology of a diverse amphibian assemblage in response to meteorological conditions / T.L. Plenderleith, et.al. *International Journal of Biometeorology*.(2018). 62:873–882. <https://doi.org/10.1007/s00484-017-1490-2>.
- [4] Y.H. Fu, et al. Declining global warming effects on the phenology of Spring leaf unfolding. *Letter*. 2015. Vol 526. *Nature* / doi:10.1038/nature15402.
- [5] P.M. Mazurkin. Method of identification.(2014). International Multidisciplinary Scientific GeoConference Surveying Geology and Mining Ecology Management. *SGEM*. 1. pp. 427-434.
- [6] P.M. Mazurkin. Wavelet Analysis Statistical Data. *Advances in Sciences and Humanities*. Vol. 1.No. 2. 2015. pp. 30-44. doi: 10.11648/j.ash.20150102.11.
- [7] P.M. Mazurkin. A.I. Kudryashova. Factor analysis of annual global carbon dynamics (according to Global_Carbon_Budget_2017v1.3.xlsx). *Materials of the International Conference "Research transfer" - Reports in English* (part 2). November 28. 2018. Beijing. PRC. P.192-224.
- [8] Mapping tree density at a global scale / T. W. Crowther. et. al. *Nature* 525.201–205 (2015); doi:10.1038/nature14967. 13 p.
- [9] C.A. Polgar, R.B. Primack. Leaf-out phenology of temperate woody plants: from trees to ecosystems // *New Phytologist* (2011) 191: 926–941. doi: 10.1111/j.1469-8137.2011.03803
- [10] M. Rousi, J. Pusenius/ Variations in phenology and growth of European white birch (*Betula Pendula*) clones // 2005. *Heron Publishing—Victoria, Canada*. *Tree Physiology* 25, 201–210/
- [11] Sellin A. et al. Elevated air humidity affects hydraulic traits and tree size but not biomass allocation in young silver birches (*Betula pendula*). *Frontiers in Plant Science*. October 2015 | Volume 6 | Article 860. doi: 10.3389/fpls.2015.00860.
- [12] Tree rings reveal globally coherent signature of cosmogenic radiocarbon events in 774 and 993 CE / U. Büntgen. et al. *NATURE COMMUNICATIONS* | (2018) 9:3605 | DOI: 10.1038/s41467-018-06036-0. 7 p.
- [13] Wang Y. et al. Thermal comfort in urban green spaces: a survey on a Dutch university campus. *Int J Biometeorol* (2017) 61:87–101. DOI 10.1007/s00484-016-1193-0.
- [14] Wang H. et al. Impacts of global warming on phenology of spring leaf unfolding remain stable in the long run. *Int J Biometeorol* (2017) 61:287–292. DOI 10.1007/s00484-016-1210-3.
- [15] Y. Zhang, L. Bielory, P. Georgopoulos. Climate change effect on *Betula*(birch) and *Quercus*(oak) pollen seasons in US // *Int J Biometeorol*. 2014 July; 58(5): 909–919. doi:10.1007/s00484-013-0674-7.

Regularities of the Dynamics of the Average Width of the Leaves of Silver Birch Near the Maximum Growth in the Vegetation Period

Mazurkin P.M.¹, Kudryashova A.I.².

¹Dr. Sc., Prof., Volga State University of Technology, Yoshkar-Ola, Russia, e - mail:

²S. lec., Volga State University of Technology, Yoshkar-Ola, Russia, e - mail:

kaf_po@mail.ru; Little-one7@yandex.ru

ABSTRACT

It is shown that the achievement of the maximum of the average width of the birch leaves is a great bioindicator of environmental quality. Moreover, the quality assessment can be carried out without measuring the concentration of pollution. According to patent 2606189 for the invention on the side at an altitude of 1.5 -2.0 m from the prevailing winds on the dynamics from July 27 to September 23, 2018, the average width of 10 leaves near the road was measured. The parameters of the model with two components showed that the half-period of oscillation at the beginning of the growing season for 10 birches varies from 1.32 to 21.35 days. All models of dynamics are the same in design, but have a different character. The growing season near the maximum growth affects with a correlation coefficient of more than 0.999, so the behavior of 10 leaves has a high quantum certainty. To assess the behavior of groups of leaves, a new criterion was introduced – the coefficient of dynamism equal to the ratio of the difference between the fact and the trend to the fact of the average width of the leaves of the birch. The maximum width of the leaves and gave the highest values of the coefficient of dynamism. This criterion allows to rank the birch in descending order of the influence of vibrations from affecting the surrounding of the birch environment.

Key words: vegetation, prevailing winds, 10 birch, 10 account of leaves, width, dynamics, oscillatory adaptation, the dynamic factor, patterns

1 Introduction

The evolution of the earth's climate for geological terms is largely due to variations in total solar radiation [13] and changes in the content of greenhouse gases in the atmosphere. Climate change affects the vegetation of the Earth [1].

The expansion of terrestrial plants, together with the ocean, has made it possible to ensure long-term habitability on the planet. Mankind uses fossil fuels, by the middle of the XXI century, the value of CO₂ will be the same as the early Eocene (50 million years ago). If the CO₂ concentration continues to rise in the XXIII century, the earth will react as one and a half billion years [3].

Understanding the response of plants to environmental factors is necessary to predict changes in the rate of carbon uptake in forests under different environmental conditions. In Finland, there is an indication of the reaction of young deciduous trees to rising air temperatures in interaction with tropospheric ozone. This knowledge increases the chances of developing models to include parameters

that describe the forest system in changing climatic conditions [8]. It can be argued that the future of CO₂ containment lies in increasing the area, primarily forests [9, 12].

The temperature dynamics [2] can be described by a set of asymmetric wavelets (a set of quanta of behavior) up to the measurement error. Similarly, the CO₂ content in the atmosphere is well quantized. The dynamics of carbon in Europe changes according to wavelets of universal design [6, 7]. Forecast V. Zharkova [14] on small ice age in the 2030-2040 is confirmed. It will start in 2032 and continue until 2046.

In ecological technologies with the use of birch leaves gradually comes the understanding of the need to simulate the mutual relations between the parameters of the structure of plant leaves by identification [4-6]. This invention relates to the engineering of biology and bioindication of the environment quality measurements of the growth of the organs of different plant species, mostly woody plants, for example, samples in the form of leaves of birch trees without cutting them with a simple and small leaf blades.

The purpose of the article is to improve the accuracy of the indication of the quality of the surrounding birch leaves of the local environment under patent 2606189 for the invention on the side at an altitude of 1.5 -2.0 m from the prevailing winds over the dynamics from July 27 to September 23, 2018, the average width of 10 leaves near the road with heavy traffic cars.

2 Materials and methods

Plant growth is a complex process, it is based on such fundamental phenomena as rhythm, polarity, differentiation, irritability, correlation. These processes are common for ontogenesis of living organisms. Ontogenesis – individual development of the body from zygote (or vegetative germ) to natural death. Thanks to the active activity of meristems and photosynthetic activity of leaves, the green plant acquires a number of features that characterize its growth. In the process of plant ontogenesis growth is observed during the main stages of its life cycle [10, 11, 14]. Therefore, in further studies it is possible to identify patterns of influence of meteorological parameters on the dynamics of vegetative organs of plants.

Table 1 shows the average widths for 10 leaves taken without cutting and measured from 27 July to 23 September 2018. A total of 18 rows. The first point on may 01 in 2018 was the beginning of the growing season, so put 0.

Table 1. The average width of 10 leaves of birch hanging for Yoshkar-Ola

Date	Time t, day	Lebedev Street	Voskresensky prospect	Street Eshkinina	Lenin avenue	Chawain Boulevard	Panfilov Street	K.Marx Street	Builders Street	Botanical garden	Osipenko Street
01.05	0	0	0	0	0	0	0	0	0	0	0
15.07	75	36.20	36.27	35.80	34.46	37.75	35.50	38.70	35.94	39.42	43.17
22.07	82	37.83	38.03	37.81	35.92	38.78	36.15	40.95	37.95	39.48	43.30
25.07	85	39.81	39.46	38.93	36.66	39.89	37.63	42.18	39.23	40.09	43.32
29.07	89	40.95	40.26	39.64	37.34	40.52	38.12	42.46	40.16	40.13	43.66
1.08	92	42.71	41.57	39.77	38.16	41.45	38.89	42.72	40.55	40.26	43.74
5.08	96	43.11	43.18	39.38	38.99	42.38	39.21	44.00	41.44	40.39	43.77
8.08	99	43.81	44.18	38.99	40.11	43.14	39.10	44.39	41.69	40.53	44.09
12.08	103	44.77	45.97	38.24	40.00	44.45	39.56	44.05	42.25	40.71	43.93
15.08	106	45.38	47.87	36.71	39.61	44.71	38.61	42.49	41.17	40.70	43.83
19.08	110	45.92	48.66	36.30	39.29	43.75	38.29	42.26	40.86	40.47	43.78
22.08	113	45.81	47.38	36.03	39.16	42.90	38.22	42.11	40.34	40.30	43.50

26.08	117	44.88	46.07	35.96	38.74	42.43	38.17	42.02	40.32	40.19	43.32
29.08	120	44.35	45.09	35.95	38.32	42.16	38.10	41.90	40.20	40.09	43.16
2.09	124	44.08	44.47	35.86	38.21	41.12	38.01	41.71	40.17	40.02	42.93
9.09	131	42.94	44.09	35.83	38.09	40.73	37.91	41.71	40.17	39.98	42.86
16.09	138	42.03	43.28	35.78	37.72	39.67	37.81	41.64	40.17	39.89	42.82
23.09	145	41.02	41.89	35.40	37.47	38.33	37.62	41.50	40.06	39.70	42.54

Note. The maximum average width values are shown in bold.

Fluctuations, in particular trends, are recorded by the wave formula [5, 6] of the form

$$y_i = A_i \cos(\pi x / p_i - a_{8i}), A_i = a_{1i} x^{a_{2i}} \exp(-a_{3i} x^{a_{4i}}), p_i = a_{5i} + a_{6i} x^{a_{7i}}, \tag{1}$$

where y – the index (dependent factor), i – number components of the model (1), m – number of members in the model (1), x – explanatory variable (influencing factor), $a_1...a_8$ – the parameters of the model (1) taking the numerical values in the course of structural-parametric identification in the software environment Curve Expert-1.40 (URL: <http://www.curveexpert.net/>), A_i – amplitude (half) of wavelet (axis y), p_i – the half-period fluctuations (axis x).

We exclude the measure of significance 0.05% [15] and estimate the adequacy of the formulas by the correlation coefficient. All 10 statistical models came out with the adequacy of the above 0.999. Therefore, the dynamics of growth and decline of leaves has a high quantum certainty.

3 Results and discussion

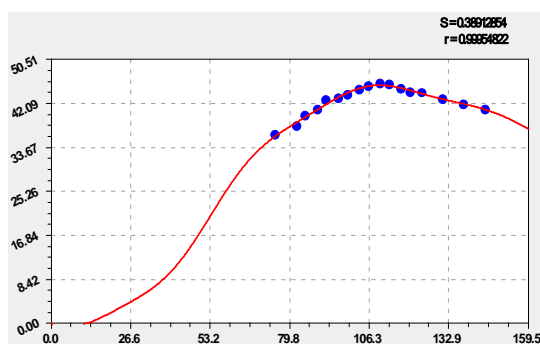
Table 2 shows the parameters of the model (1) with two components, the first of which is a trend in the form of biotechnical law [4]. Cyclical fluctuations in 01.05.2018. halftime shows a_{5i} . The half-period of oscillation at the beginning of the growing season for 10 birches varies from 1.32 (Panfilov street) to 21.35 days (Lebedev street).

Table 2. Models (1) dynamics of average width of birch leaves

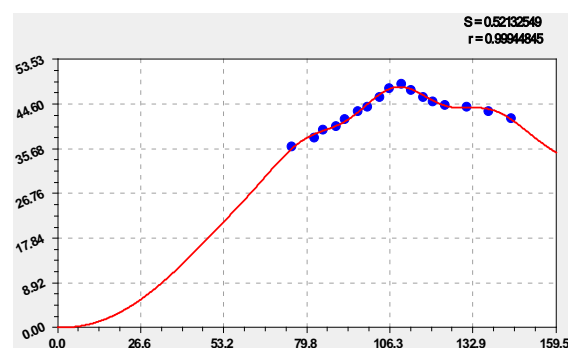
Number i	Wavelet $y_i = a_{1i} x^{a_{2i}} \exp(-a_{3i} x^{a_{4i}}) \cos(\pi x / (a_{5i} + a_{6i} x^{a_{7i}}) - a_{8i})$								Coef. corr. r
	The amplitude (half) the fluctuations				The half-period of oscillations			Shift	
	a_{1i}	a_{2i}	a_{3i}	a_{4i}	a_{5i}	a_{6i}	a_{7i}	a_{8i}	
Lebedev Street									
1	1.21685e-5	9.17015	6.05278	0.32571	0	0	0	0	0.9995
2	0.44598	0.48964	0.048008	0.79134	21.25481	0	0	-2.85512	
Voskresensky prospect									
1	0.0040275	2.23873	0.00027388	1.77914	0	0	0	0	0.9994
2	-1.06631e-22	13.60735	0.074901	1.09307	18.25100	-4.10921e-5	1.86324	-3.10286	
Street Eshkinina									
1	4.37213e7	6.24840	21.67608	0.14738	0	0	0	0	0.9998
2	-0.27508e-17	11.50074	0.27033	0.85753	9.26474	0.0010104	1.76082	-4.63677	
Lenin avenue									
1	0.021506	2.08161	0.035573	0.88346	0	0	0	0	0.9999
2	-2.56548e-24	14.15017	0.17309	0.90399	1.55507	0.0029436	1.41184	4.23812	
Chawain Boulevard									

1	0.079922	1.54159	0.00039496	1.65732	0	0	0	0	0.9997
2	-4.74722e-30	17.78349	0.055937	1.20232	14.57925	0.00056749	1.68957	-1.52615	
Panfilov Street									
1	3.66251e6	7.38171	21.73815	0.16016	0	0	0	0	0.9998
2	-1.03801	1.08360	1.48447	0.27784	1.31728	0.023483	1.07558	0.91434	
Karl Marx Street									
1	1.31774e6	7.87565	21.57557	0.16721	0	0	0	0	0.9994
2	-5.06517e-6	4.54130	0.83355	0.50876	15.76053	0.00020116	1.98175	-4.85485	
Builders Street									
1	1.86986e6	9.10854	24.13993	0.16944	0	0	0	0	0.9998
2	-7.26191e-19	11.79845	0.26301	0.83912	13.57641	0.0017335	1.61783	-3.64787	
Botanical garden									
1	6.59123	0.52516	0.013763	0.82177	0	0	0	0	1.0000
2	-1.28495e-21	12.70989	0.13276	0.97603	20.55353	0.00012933	1.60894	-0.35495	
Osipenko Street									
1	8.05960e8	3.85974	20.58087	0.11220	0	0	0	0	1.0000
2	-0.049369	0.83696	1.13220	0.15655	9.57983	0.10275	0.82053	-5.58996	

Figures 1 and 2 show the graphs of the two-term formula according to table 2. They are all the same in design, but have different patterns of change over time. Then it can be argued that the dynamics of the parameters of birch leaves hanging during the growing season near the maximum increment is very highly adequate with a correlation coefficient of more than 0.999, that is, the average behavior of 10 leaves has a quantum certainty. But meteorological parameters during the growing season of the birch have a strong quantum entanglement. Then in the future it is necessary to understand how the birch leaves for 180 million. have years of evolution gained such high vibrational adaptability? It feels as if they understand and lead their vegetative organs consciously to changes in the surrounding group of accounting leaves environment.



Lebedev Street



Voskresensky prospect

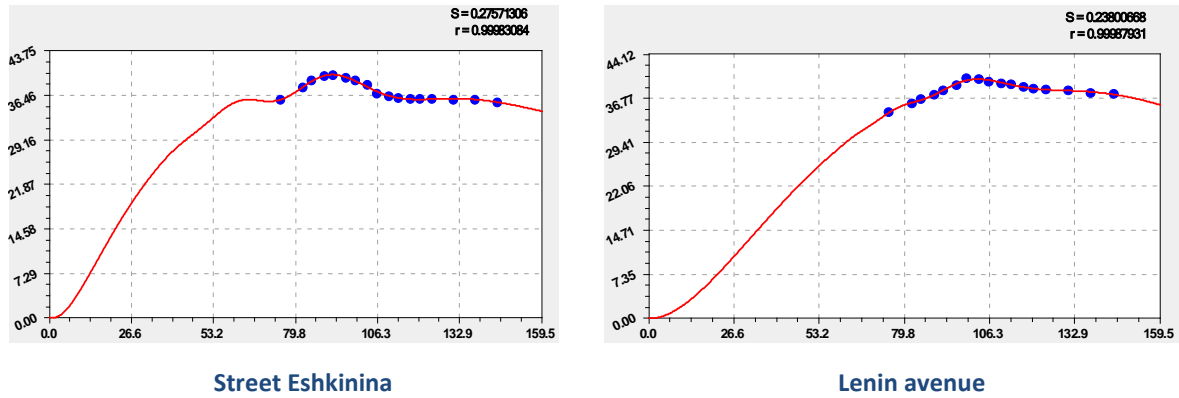


Figure 1. Graphs of the dynamics of the average width of the group of 10 leaves of birch

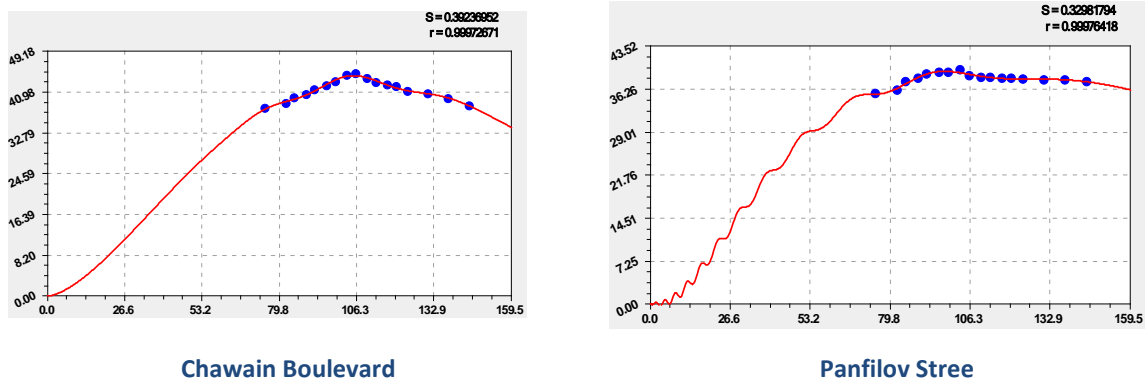
To assess the behavior of leaf groups, we introduce a new criterion – the coefficient of dynamism equal to the ratio of the difference between the fact and the trend to the fact of the average width (table. 3). The maximum width of the leaves and gave the highest values of the coefficient of dynamism.

Table 3. The coefficient of dynamic growth of the leaves of the silver birch

Date	Time t, day	Lebedev Street	Voskresensky prospect	Street Eshkinina	Lenin avenue	Chawain Boulevard	Panfilov Street	K.Marx Street	Builders Street	Botanical garden	Osipenko Street
01.05	0	-	-	-	-	-	-	-	-	-	-
15.07	75	0.0127	0.0331	-0.0371	0.0050	0.0078	-0.0098	-0.0281	-0.0151	-0.0007	0.0007
22.07	82	-0.0336	-0.0168	0.0028	-0.0069	-0.0224	-0.0259	-0.0064	-0.0090	-0.0097	-0.0046
25.07	85	-0.0123	-0.0143	0.0274	-0.0050	-0.0134	0.0035	0.0118	0.0079	0.0022	-0.0065
29.07	89	-0.0176	-0.0344	0.0414	-0.0076	-0.0194	0.0043	0.0064	0.0133	-0.0005	-0.0009
1.08	92	0.0041	-0.0275	0.0431	0.0009	-0.0098	0.0169	0.0054	0.0119	0.0005	-0.0002
5.08	96	-0.0084	-0.0174	0.0333	0.0078	-0.0013	0.0177	0.0276	0.0217	0.0015	-0.0001
8.08	99	-0.0048	-0.0115	0.0244	0.0270	0.0089	0.0110	0.0327	0.0209	0.0038	0.0072
12.08	103	0.0047	0.0106	0.0076	0.0155	0.0317	0.0189	0.0224	0.0275	0.0073	0.0042
15.08	106	0.0122	0.0408	-0.0311	0.0009	0.0348	-0.0067	-0.0142	-0.0014	0.0068	0.0028
19.08	110	0.0198	0.0487	-0.0381	-0.0115	0.0134	-0.0155	-0.0191	-0.0115	0.0013	0.0033
22.08	113	0.0170	0.0203	-0.0417	-0.0165	-0.0041	-0.0167	-0.0211	-0.0250	-0.0024	-0.0015
26.08	117	-0.0007	-0.0068	-0.0372	-0.0276	-0.0095	-0.0158	-0.0197	-0.0244	-0.0039	-0.0032
29.08	120	-0.0084	-0.0249	-0.0320	-0.0375	-0.0096	-0.0151	-0.0190	-0.0254	-0.0052	-0.0047
2.09	124	-0.0061	-0.0300	-0.0266	-0.0368	-0.0238	-0.0131	-0.0176	-0.0221	-0.0050	-0.0068
9.09	131	-0.0108	-0.0121	-0.0119	-0.0289	-0.0068	-0.0054	-0.0044	-0.0114	-0.0015	-0.0019
16.09	138	-0.0031	0.0082	0.0039	-0.0226	0.0015	0.0050	0.0101	0.0031	0.0020	0.0045
23.09	145	0.0083	0.0262	0.0120	-0.0085	0.0096	0.0154	0.0253	0.0179	0.0040	0.0061

Note. The maximum dynamic factor values are shown in bold.

This criterion allows to rank the birch in descending order of the influence of fluctuations.



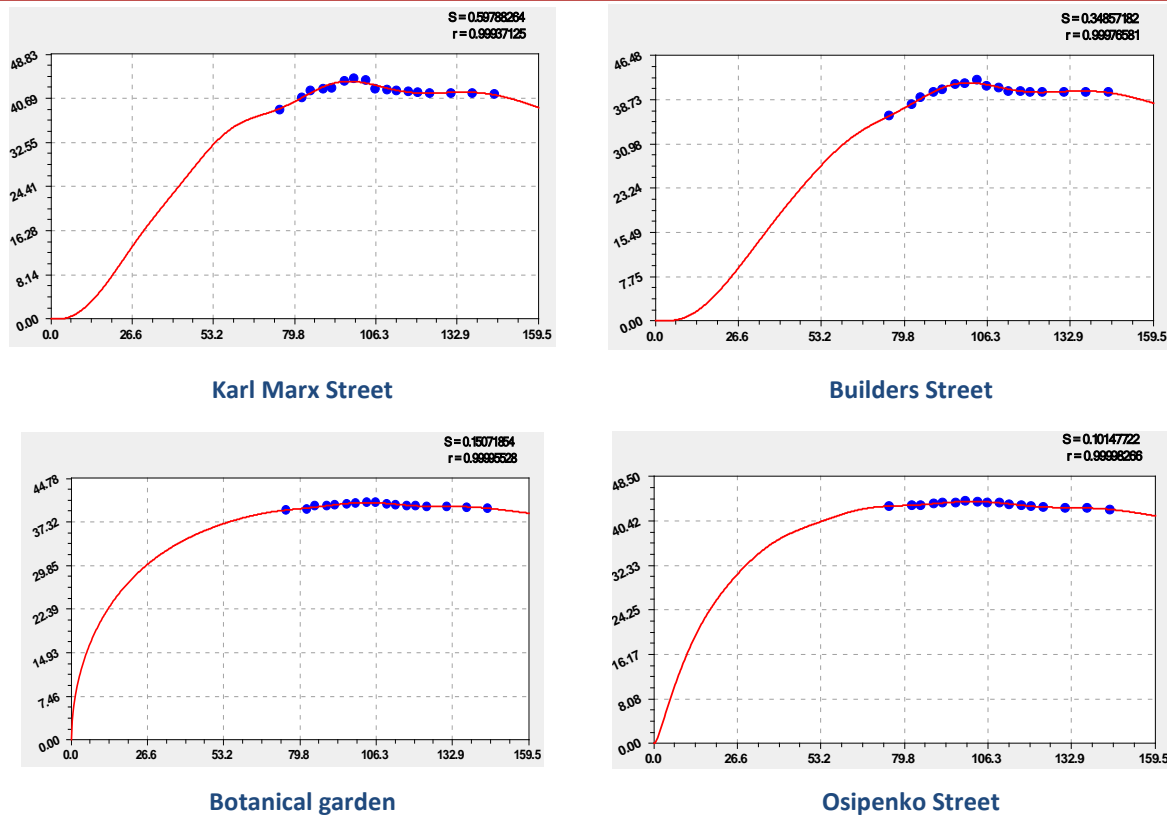


Figure 2. Graphs of the dynamics of the average width of the group of 10 leaves of birch

According to table 3, places for deterioration of conditions are distributed as follows: 1) 0.0072 – Osipenko street, where there are almost no cars; 2) 0.0073 – Botanical garden, very little influence of the fence around the object; 3) 0.0189 – Panfilov street; 4) 0.0198 – Lebedev street; 5) 0.0270 – Lenin Avenue; 6) 0.0275 – Builders street; 7) 0.0327 – Karl Marx street; 8) 0.0438 – chavain Boulevard; 9) 0.0431 – Eshkinina street; 10) 0.0487 – Voskresensky Prospect.

So what is better, a quiet life with a low coefficient of dynamism, or the largest increment of the average width of the leaves of birch hanging? On average the maximum width of the sheet from the table, 1 birch in the deterioration of productivity is as follows: 1) 48.66 mm – Voskresensky prospect; 2) 45.92 mm is the street Lebedev; 3) 44.71 mm Boulevard chavajjna; 4) 44.39 mm – street Karla Marksa; 5) 44.09 mm – Osipenko street; 6) 42.25 mm – the street of Builders, 7) 40.71 mm – Botanical garden; 8) 40.11 mm – Prospekt Laziness-on; 9) 39.77 mm street Eshkinina; 10) 39.56 mm – Panfilov's street. Of course, the growth of increments and the achievement of the average maximum width of the leaves affects the own physiological state of the tree. For example, a birch with productive leaves according to table 1 for four days from 15.08 to 19.08 changed the average width of leaves on Voskresensky Avenue from 47.87 to 48.66 mm or had an increment rate $(48.66 - 47.87) / 4 = 0.198$ mm. And on Panfilov street the average growth rate of leaf width is $(39.56 - 39.10) / 4 = 0.115$ mm.

As is known, environmental monitoring is carried out for a variety of types of pollution, the content of which in air, water and soil should not exceed the maximum permissible concentrations. However, indirect monitoring through the behavior of birch leaves hanging in the growing season allows without measuring the concentrations of pollution to conduct an environmental assessment of the territory of the place of growth of the birch. As a result, birch leaves react to all changes in the environment of birch, and take into account the effects that are still unknown to man. This is the essence of our methods of environmental indication and patent 2606189 becomes a pioneering solution.

To be accepted as criteria for the environmental assessment of the rate of increment, it is necessary to take into account the physiological parameters of the tree, for example, classes of sanitary state, age and more. Thus, to indicate the environment around birch's recommended ratio of dynamism, with a maximum of medium size account leaves.

4 Conclusion

The 2606189 patent for invention from the side at a height of 1.5 to 2.0 m from the side of the prevailing winds on the dynamics from 27 July to 23 September 2018 measured average width of 10 account leaves around the road. The parameters of the model with two components showed that the half-period of oscillation at the beginning of the growing season for 10 birches varies from 1.32 to 21.35 days. All models of dynamics are the same in design, but have a different character. The growing season near the maximum growth affects with a correlation coefficient of more than 0.999, so the behavior of 10 leaves has quantum certainty.

To evaluate the behavior of leaf groups, a new criterion is introduced – the coefficient of dynamism equal to the ratio of the difference between the fact and the trend to the fact of the average width. The maximum width of the leaves and gave the highest values of the coefficient of dynamism. This criterion allows to rank the birch in descending order of the influence of vibration influence of the environment.

REFERENCES

- [1] Korona V. V., Vasilyev A. G. Structure and variability of plant leaves: fundamentals of modular theory. *Ekaterinburg: Uro ran*, 2007. 280 PP.
- [2] Mazurkin P. M., Kudryashova A. I. Quanta of behavior of meteorological parameters on three-hour measurements in the growing season of birch // *American Scientific Journal* № (24) / 2019. P. 59-75.
- [3] Foster G.L., Royer D.L., Lunt D.J. Future climate forcing potentially without precedent in the last 420 million years // 2017. *Nature communications* | 8:14845 | DOI: 10.1038/ncomms14845 | www.nature.com/naturecommunications.
- [4] Mazurkin P.M. Method of identification. (2014). International Multidisciplinary Scientific GeoConference Surveying Geology and Mining Ecology Management, *SGEM*, 1 (6), pp. 427-434. <https://www.scopus.com/inward/record.uri?eid=2-s2.0-84946541076&partnerID=40&md5=72a3fcce31b20f2e63e4f23e9a8a40e3>
- [5] Mazurkin P.M. Identification of the wave patterns of behavior. (2014). International Multidisciplinary Scientific GeoConference Surveying Geology and Mining Ecology Management, *SGEM*, 1 (6), pp. 373-380. <https://www.scopus.com/inward/record.uri?eid=2-s2.0-84946550468&partnerID=40&md5=0fd8f91ed5b1f0592fc587e5ffb14e51>
- [6] Mazurkin. P.M. Wavelet Analysis Statistical Data. *Advances in Sciences and Humanities*. Vol. 1, No. 2, 2015, pp. 30-44. doi: 10.11648/j.ash.20150102.11.
- [7] Mazurkin P.M., Kudryashova A.I.. Factor analysis of annual global carbon dynamics (according to Global_Carbon_Budget_2017v1.3.xlsx). *Materials of the International Conference "Research transfer" - Reports in English* (part 2). November 28, 2018. Beijing, PRC. P.192-224.

- [8] Maarit M. Impacts of temperature and ozone on carbon retention processes of birch and aspen *Dissertations in Forestry and Natural Sciences*. Finland, Joensuu, on June, 08, 2012, 54 p.
- [9] Mapping tree density at a global scale / T. W. Crowther, et. al. *Nature* 525, 201–205 (2015); doi:10.1038/nature14967. 13 p.
- [10] Polgar C.A., Primack R.B. Leaf-out phenology of temperate woody plants: from trees to ecosystems // *New Phytologist* (2011) 191: 926–941. doi: 10.1111/j.1469-8137.2011.03803
- [11] Rousi M., Pusenius J. / Variations in phenology and growth of European white birch (*Betula Pendula*) clones // 2005. *Heron Publishing—Victoria, Canada*. *Tree Physiology* 25, 201–210.
- [12] Tree rings reveal globally coherent signature of cosmogenic radiocarbon events in 774 and 993 CE / U. Büntgen, et al. *NATURE COMMUNICATIONS* | (2018) 9:3605 | DOI: 10.1038/s41467-018-06036-0. 7 p.
- [13] Zharkova V.: the solar magnet field and the terrestrial climate. URL: <https://watchers.news/2018/11/11/valentina-zharkova-solar-magnet-field-and-terrestrial-climate-presentation/> (Дата обращения 01.03.2019).
- [14] Zhang Y., Bielory L., Georgopoulos P.. Climate change effect on *Betula* (birch) and *Quercus* (oak) pollen seasons in US // *Int J Biometeorol*. 2014 July; 58(5): 909–919. doi:10.1007/s00484-013-0674-7.
- [15] Wasserstein L.R., et.al. (2019). Moving to a World Beyond “ $p < 0.05$ ”, *The American Statistician*, 73:sup1, 1-19, DOI: 10.1080/00031305.2019.1583913.

Improving Dynamic Parallel MRI Reconstruction via a Kernel-Based Learning Technique

¹Yuchou Chang

¹Computer Science and Engineering Technology Department, University of Houston-Downtown,
Houston, Texas, United States
changy@uhd.edu

ABSTRACT

As an important radiology technology, magnetic resonance imaging (MRI) has been widely used in clinical applications. However, its low imaging speed restricts some clinical applications such as dynamic imaging. Parallel MRI was proposed to accelerate imaging speed by undersampling k-space data and applied on dynamic imaging like cardiac imaging. Due to undersampled k-space data, noise is a problem in reconstructed MR images. We propose a nonlinear technique to improve a temporal parallel MRI reconstruction method. Experimental results show that the proposed nonlinear technique outperforms the traditional method.

Keywords: Kernel Method; Parallel MRI; Dynamic MRI; Reconstruction; Noise Reduction.

1 Introduction

Magnetic resonance imaging (MRI) [1] uses the principle of nuclear magnetic resonance and a gradient magnetic field to detect the emitted electromagnetic waves. It can be used to draw structural images inside the object. Magnetic resonance imaging has been widely used in physics, medicine, food and agriculture, and other fields. Magnetic resonance imaging is a technique for imaging human body using the principle of nuclear magnetic resonance. It can accurately obtain the physiological functions, anatomical structures, and lesion information of human tissues and organs. It has become one of the important methods of medical diagnosis. MRI is limited by the Nyquist sampling theorem, so traditional magnetic resonance imaging has a longer scanning time and slower imaging speed, which cannot meet the requirements of high-speed clinical applications such as real-time cardiac imaging. Parallel magnetic resonance imaging is a method of simultaneously acquiring signals by using multiple receiving coils, reducing the number of phase encodings required when a single coil is used, thereby reducing signal acquisition time and speeding up imaging speed. It undersamples k-space data, which greatly shortens the magnetic resonance scanning time and improves the imaging speed. The major reconstruction algorithms are GRAPPA [2] and SENSE [3]. GRAPPA is a reconstruction algorithm based on k-space, and SENSE is based on image domain.

Magnetic resonance imaging usually requires a long scan time, especially for dynamic applications such as real-time cardiac imaging to meet the requirements of clinical applications. Long time scanning has restricted the wide clinical applications of magnetic resonance imaging. Dynamic magnetic resonance imaging can be sparsely represented, which provides conditions for the application of compressed sensing. Real-time dynamic magnetic resonance imaging technology is desired for cardiac imaging. Temporal GRAPPA [4] is applied on real-time cardiac imaging with an interleaved acquisition scheme.

The main idea of the kernel method [5, 6] is based on the assumption that a set of points which cannot be linearly classified in a low-dimensional space is likely to become linearly separable when they are transformed into a set of points in a high-dimensional space. High-dimensional mapping solves problems that are difficult to classify datasets in low-dimensional and original space. However, if low-dimensional data is directly converted into a high-dimensional space and then linear classification plane is searched, there are two problems. Firstly, it is the curse of dimension problem in high-dimensional space. Secondly, since each point needs to be converted to a high-dimensional space, and then the parameters of the classification plane are calculated, therefore it is a long time procedure. Kernel trick solves those two problems without explicit mapping on data. Kernel method has been used in parallel MRI reconstruction for accelerating imaging speed and enhancing imaging quality. Kernel method has been used for parallel MRI reconstruction [7, 8]. It has some advantages like suppressing noise as well as keeping high speed of imaging. For temporal GRAPPA, it may be improved by kernel method. In this paper, we propose to use kernel method on temporal GRAPPA for improving reconstruction quality. The first part is the introduction. The second part will give the proposed method. Experimental results and conclusion are given in the third and the fourth parts.

2 The Proposed Method

Magnetic resonance imaging is a non-invasive imaging technique. In compared with X-ray or computed tomography, the advantage of magnetic resonance imaging is its safety, accuracy, and non-radiation. However, MRI has a slower imaging speed. Parallel imaging method avoids limitations of traditional magnetic resonance imaging by skipping acquisition of k-space. GRAPPA is a widely used parallel MRI technique [2]. For the GRAPPA method, the whole k-space is undersampled with equivalent distance along phase-encoding direction. In addition, extra data are acquired in the center k-space as auto-calibration signal (ACS) data. ACS data are used to calculate fitting coefficients at first and then missing data are estimated with calculated coefficients and undersampled data to obtain complete k-space data. Finally, inverse Fourier transform is applied on each coil's k-space data and then all coil images are combined to obtain a reconstructed image. Some parameters including fitting mask, number of ACS lines, number of coils, and reduction factor of undersampled k-space data determine the reconstruction quality and speed.

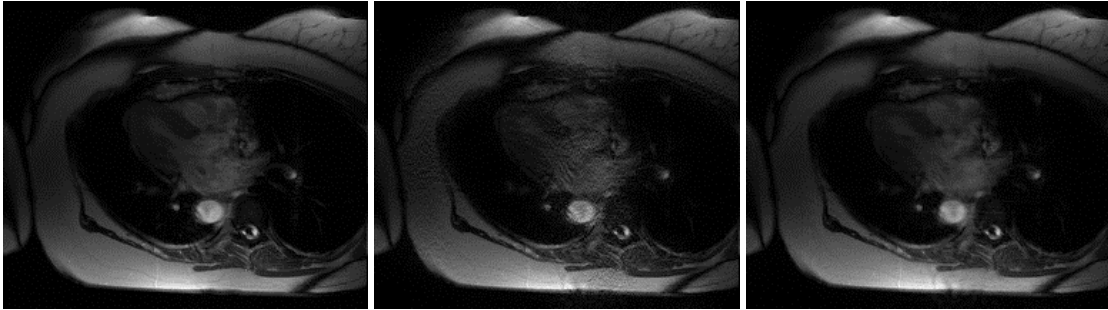
Nonlinear GRAPPA [7] is an extension of the traditional GRAPPA method. A polynomial kernel is incorporated into coefficient calculation and missing data estimation procedures. Nonlinear mapping is given to build a relationship between missing data and undersampled k-space data, so that it is more accurate than linear mapping as used in the traditional GRAPPA. Kernel methods are a class of algorithms for machine learning and pattern recognition. The general task is finding general relationships in data. Kernel methods transform data from low-dimensional space to higher-dimensional space. Data can be more easily separated or modeled in high-dimensional space. The transformation may lead to infinite dimensional space. Furthermore, temporal GRAPPA (TGRAPPA) [4] uses an interleaved acquisition scheme to build a new set of ACS lines for reconstructing the next frame in dynamic imaging.

In the proposed method, TGRAPPA is improved by nonlinear fitting and estimation technique for accurately reconstructing missing k-space data. The nonlinear formulation is derived from polynomial kernel format as used in nonlinear GRAPPA reconstruction [7]. Kernel method has been widely used in machine learning technique like support vector machine (SVM). It maps data from linear space to feature space via a kernel. They are different types of kernel including polynomial kernel, Gaussian kernel, and so forth. ACS data can be considered in a traditional linear space and it can be transformed into feature space via a kernel. We apply polynomial kernel to transform the new set of ACS data in

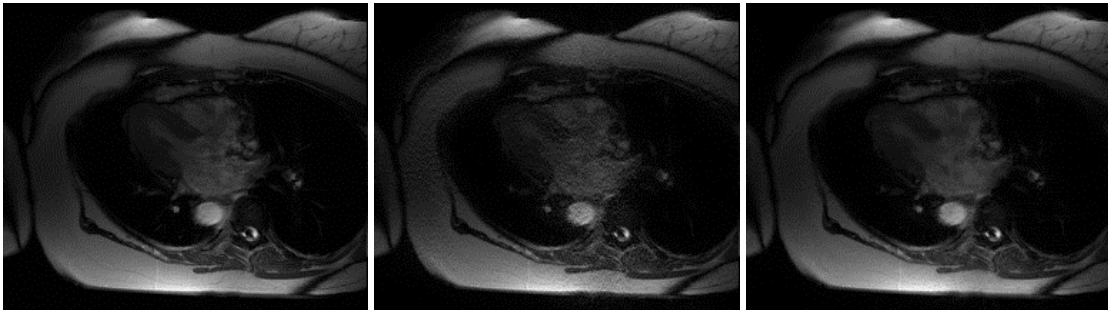
TGRAPPA into feature space and then use them to reconstruct missing data in a series of undersampled k-space. The nonlinear TGRAPPA has a nonlinear fitting and estimating process in compared to traditional TGRAPPA.

3 Experimental Results

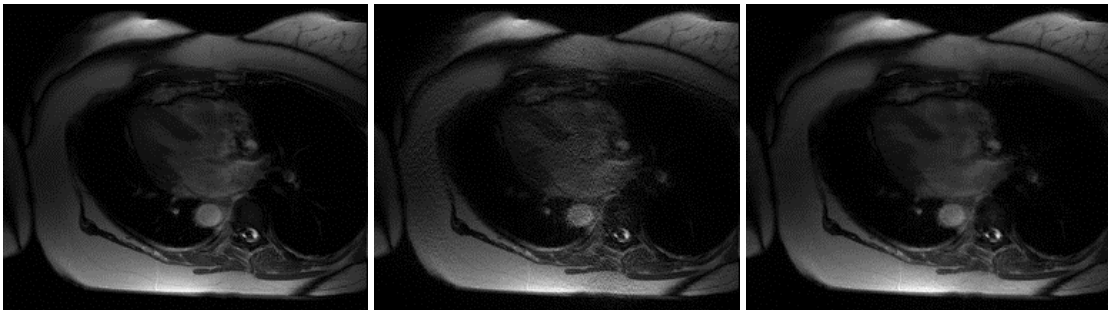
The proposed nonlinear TGRAPPA is evaluated on a set of cardiac dataset. The fully sampled k-space data is reconstructed as reference images. In addition, traditional TGRAPPA is also compared to the proposed nonlinear TGRAPPA. For undersampling k-space data, 40 ACS lines and outer reduction factor 4 are used. The reconstruction mask uses 15 columns by 4 blocks for both of TGRAPPA and nonlinear TGRAPPA reconstruction. As shown in the Figure 1, the proposed nonlinear TGRAPPA (right column) is able to suppress noise in compared to TGRAPPA reconstructed images (middle column).



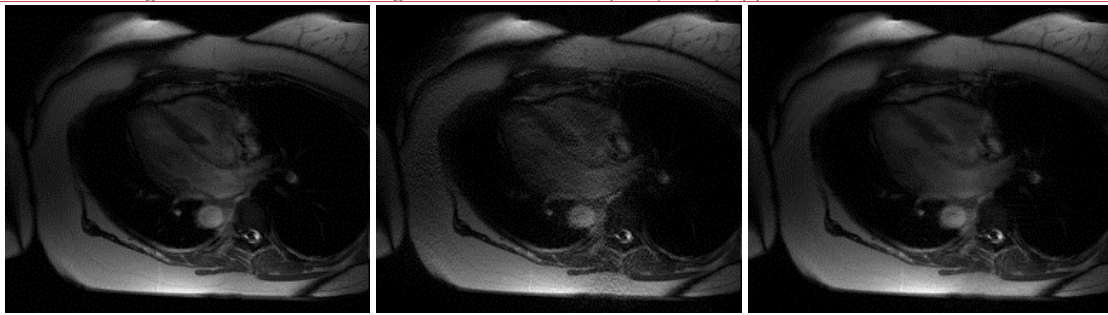
Frame 1



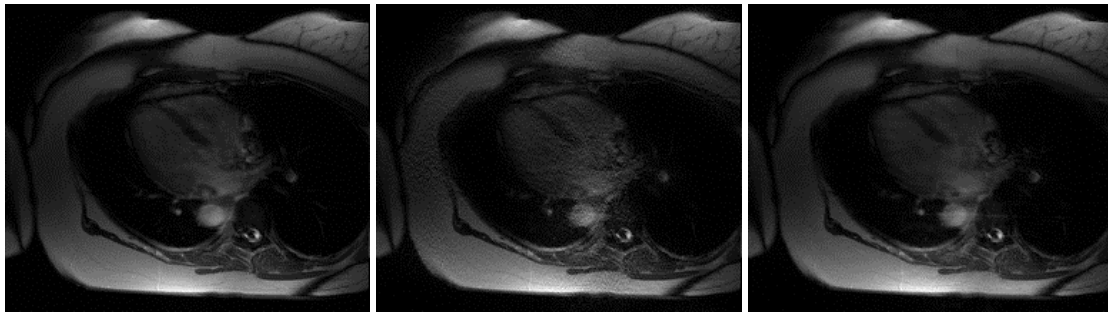
Frame 2



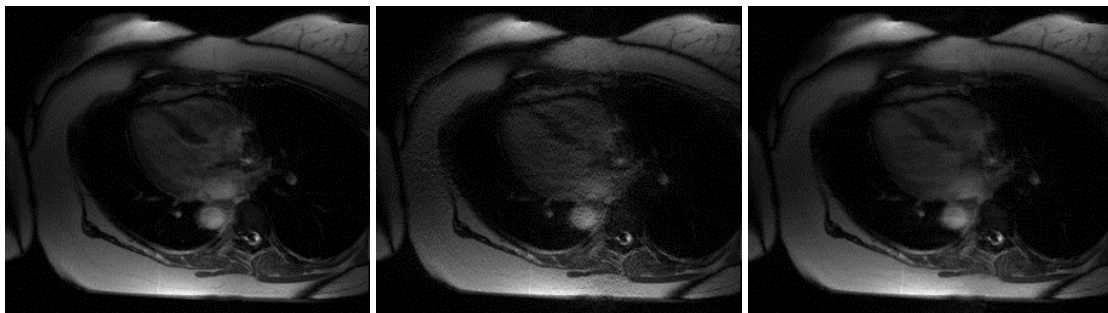
Frame 3



Frame 4



Frame 5



Frame 6

Figure 1. Six frames of a sequence of cardiac images reconstructed by fully sampled k-space data as reference (left column), TGRAPPA (middle column), and nonlinear TGRAPPA (right column).

4 Conclusion

A nonlinear reconstruction based on kernel method is proposed. It maps k-space data to feature space constructed by polynomial kernel, and then reconstruct missing k-space data in a sequence of dynamic imaging dataset. Experimental results show the proposed nonlinear method outperforms the traditional TGRAPPA by suppressing noise. Its reconstruction quality is closer to reference image reconstructed by fully sampled data.

REFERENCES

- [1] Haacke E. M., et al., *Magnetic resonance imaging: Physical principles and sequence design*. Wiley-Liss, 1st edition, 1999.
- [2] Griswold M.A., et al., *Generalized autocalibrating partially parallel acquisitions (GRAPPA)*. *Magnetic Resonance in Medicine*, 2002. 47(6): p. 1202-1210.

- [3] Pruessmann K.P., et al., *SENSE: sensitivity encoding for fast MRI*. Magnetic Resonance in Medicine, 1999. 42(5): p. 952-962.
- [4] Breuer F.A., et al., *Dynamic autocalibrated parallel imaging using temporal GRAPPA (TGRAPPA)*. Magnetic Resonance in Medicine, 2005. 53(4):981-985.
- [5] Vapnik, V., et al., *The Nature of Statistical Learning Theory*. Springer, 2nd edition, 1999.
- [6] Schölkopf, B., et al., *Learning with Kernels: Support Vector Machines, Regularization, Optimization, and Beyond*. The MIT Press, 1st edition, 2001.
- [7] Chang, Y., et al., *Nonlinear GRAPPA: a kernel approach to parallel MRI reconstruction*. Magnetic Resonance in Medicine, 2012. 68(3): p. 730-740.
- [8] Lyu J., et al., *Fast GRAPPA reconstruction with random projection*. Magnetic Resonance in Medicine, 2015. 74(1): p. 71-80.